Photosubstitution of d^6 Metal Carbonyls $M(CO)_5L$ Revisited: A Theoretical Study

T. Matsubara,† C. Daniel,* and A. Veillard

Laboratoire de Chimie Quantique, UPR 139 du CNRS, Institut Le Bel, 4 rue Blaise Pascal, F-67000 Strasbourg, France

Received May 24, 1994®

A theoretical study of the photosubstitution reactions of d^6 metal carbonyls $M(CO)_5L$, characterized by a high degree of cis stereospecificity, is reported. The possible excited-state isomerization pathways of the five-coordinate species $M(CO)_4L$ (square pyramid (SP), with L basal or apical, trigonal bipyramid regular (TBP) or distorted (d-TBP)) have been considered on the basis of CASSCF/CASPT2 calculations of the relative stabilities of the different structures of $Mn(CO)_4Cl$ in the lowest excited states (singlet or triplet). The basis set effect on the relative stabilities of the various structures of $Tc(CO)_4Cl$ and $Mo(CO)_4NH_3$ have been ascertained at the SCF level with double-ζ-quality basis sets. The results obtained for $Mn(CO)_4Cl$ have been used to generate a state correlation diagram that connects the ground state and lowest excited states of the reactant $Mn(CO)_5Cl$ with those of the five-coordinate species with different structures. On the basis of this diagram, we propose the following mechanism. (i) Excitation of $Mn(CO)_5Cl$ occurs into the ^1E ligand field state followed by elimination of a carbonyl ligand with formation of $Mn(CO)_4Cl$ either as an SP apical in the ^1E state (axial elimination) or as an SP basal in the $^1A'$ state (equatorial elimination). (ii) Through a Berry pseudorotation, followed by a $^1B_2 \rightarrow {}^1A_1$ internal conversion, the SP structures evolve either to the $^1A_1$ ground state of the regular TBP or to the d-TBP in the $^1A_1$ state. (iii) The molecule gets trapped in the potential well corresponding to the $^1A_1$ ground state of the d-TBP (after a downhill rearrangement in the case of the regular TBP), until it reacts with an incident nucleophile, leading to the cis derivatives.

Introduction

UV–vis irradiation of metal carbonyls is the method of choice for the generation of catalytically active species or for the synthesis of substituted derivatives in the presence of potential ligands. It is commonly observed that, compared with their ground-state properties, the reactivity of these compounds toward loss of CO is greatly enhanced upon electronic excitation to a ligand field excited state.[1] The mechanism of photosubstitution of these molecules has been discussed by several authors.[2,3] However, the role of the various ligand field states, the importance of the triplet states, the nature of the intermediates, and the efficiency of intersystem crossing are still a matter of debate.

The approach based on the state correlation diagrams that connect the ground and excited states of the reactant and of the primary products has enabled us to analyze the mechanism of a number of photochemical reactions of organometallics.[4,5] For instance, we have proposed a qualitative mechanism for the photosubstitution of d^6 metal carbonyls $M(CO)_5L$:

$$M(CO)_5L + L' \xrightarrow{h\nu} M(CO)_4LL' + CO \qquad (1)$$

This reaction has been found experimentally to be highly stereospecific, yielding in most cases the cis isomer.[6] There is a general agreement that a dissociative mechanism represents the primary photoprocess for carbonyl substitution:

$$M(CO)_5L \xrightarrow{h\nu} M(CO)_4L + CO \qquad (2)$$

the coordinatively unsaturated species undergo a subsequent thermal reaction:

$$M(CO)_4L + L' \rightarrow M(CO)_4LL' \qquad (3)$$

On the basis of state correlation diagrams which connect the singlet states of the various structures (square pyramidal (SP), trigonal bipyramid (TBP), and distorted trigonal bipyramid (d-TBP) of the five-coordinate model systems $M(CO)_4L$ (with M = Mo and L = NH_3, PMe_3, C(OMeH), C_2H_4 or M = Tc and L = Cl), we have proposed a mechanism for the carbonyl elimination (reaction 2).[2] This mechanism, based on ligand field excitations, accounts for the cis-stereospecificity of the photosubstitution observed for a large variety of heteroligands (halide, amide, phosphine, and some carbene groups): (i) excitation of $M(CO)_5L$ into the ^1E ligand field state is followed by elimination of one carbonyl

† Present address: The Cherry L. Emerson Center for Scientific Computation, Emory University, Atlanta, GA.

® Abstract published in *Advance ACS Abstracts,* November 1, 1994.

(1) Geoffroy, G. L.; Wrighton, M. S. *Organometallic Photochemistry*; Academic Press: New-York, 1979.

(2) Daniel, C.; Veillard, A. *Nouv. J. Chimie* **1986**, *10*, 83 and references therein.

(3) Pierloot, K.; Hoet, P.; Vanquickenborne, L. G. *J. Chem. Soc., Dalton Trans.* **1991**, 2363.

(4) Veillard, A. In *Photoprocesses in transition metal complexes, biosystems and other molecules. Experiment and theory*; Kochanski, E., Ed.; Kluwer Academic Publishers: Dordrecht, **1991**; pp 173–216.

(5) Daniel, C.; Veillard, A. In *Transition metal hydrides*; Dedieu, A., Ed.; VCH Publishers: New-York; **1992**; p 235–261.

(6) See references given in ref 2.

0276-7333/94/2313-4905$04.50/0 © 1994 American Chemical Society

ligand with the species $M(CO)_4L$ formed either as a SP in the excited state ^1E with the ligand L apical (axial elimination) or as a SP in the excited state $^1A'$ with the ligand L basal (equatorial elimination); (ii) in the case of axial elimination, rearrangement of the SP with L apical along an irreversible Berry pseudorotation path results in a SP with L basal in a $^1A'$ excited state; (iii) in both cases, the SP with L basal evolves through internal conversion to its ground state $^1A'$; (iv) $M(CO)_4L$ as a SP (with L basal) in its ground state $^1A'$ will react with an incident nucleophile L′ to give $M(CO)_4LL'$ with the cis structure.

In a recent study, Vanquickenborne *et al.* (abbreviated as PHV) used a similar approach to study the photochemical substitution of $Mn(CO)_5Cl$.[3] They relied on SCF calculations of the various structures of $Mn(CO)_4Cl$ in the ground and lowest excited states to set up a state correlation diagram. Their conclusions disagree with ours on a number of points.

(i) The relative stabilities of the various structures (SP with L basal or apical, TBP regular of distorted) are not the same and this is particularly true for the excited states; for instance, the order of decreasing stability in the lowest singlet state is d-TBP > SP basal > SP apical > TBP for $Mn(CO)_4Cl$ in PHV and d-TBP > SP basal > TBP > SP apical for $Tc(CO)_4Cl$ in the work of Daniel and Veillard (abbreviated as DV);[2] for the first excited singlet state the order is TBP > d-TBP > SP apical > SP basal for $Mn(CO)_4Cl$ in PHV and SP basal > TBP > SP apical for $Tc(CO)_4Cl$ in DV.

(ii) As a consequence, these two works also differ in the mechanism of the photochemical reaction 2 as well as to the nature of the reactive species of the nucleophilic addition reaction 3, which is postulated to be d-TBP in PHV rather than SP basal in DV. In DV, the photoelimination of a carbonyl ligand, axial or equatorial, results in the formation of the SP basal first in the excited state $^1A'$ and next in its ground state $^1A'$ through internal conversion and this SP basal will react with a nucleophile L′ according to reaction 3 (Figure 1a). In the study by PHV, after the elimination of an axial carbonyl ligand, the $Mn(CO)_4Cl$ species evolves along the excited state potential energy surface from an SP apical to a TBP and is brought by intersystem crossing from the $^1B_2$ state to the $^3B_2$ state of the TBP. Conversion to a d-TBP in its ground state $^1A_1$ occurs through a second intersystem crossing. The d-TBP then reacts with the nucleophile (Figure 1b).

(iii) The possible role of the triplet states was not considered in the work of DV since the reactant $M(CO)_5L$ is first excited in a singlet state and since the ground state of the primary product $M(CO)_4LL'$ is also a singlet state, so it was assumed that the system remains in a singlet state along the entire reaction path. On the contrary, the triplet state plays a key role in the mechanism proposed by PHV, however at the cost of two successive intersystem crossings.

The reasons for these disagreements are not clear. The metal center is different in the two studies (Tc and Mo in DV, Mn in PHV) and it is quite possible that the relative stability of the different structures and the mechanism of the photochemical substitution are not the same for metal carbonyls of the first and second transition series. Technical factors like the size of the basis sets used, the extent of geometry optimization, and

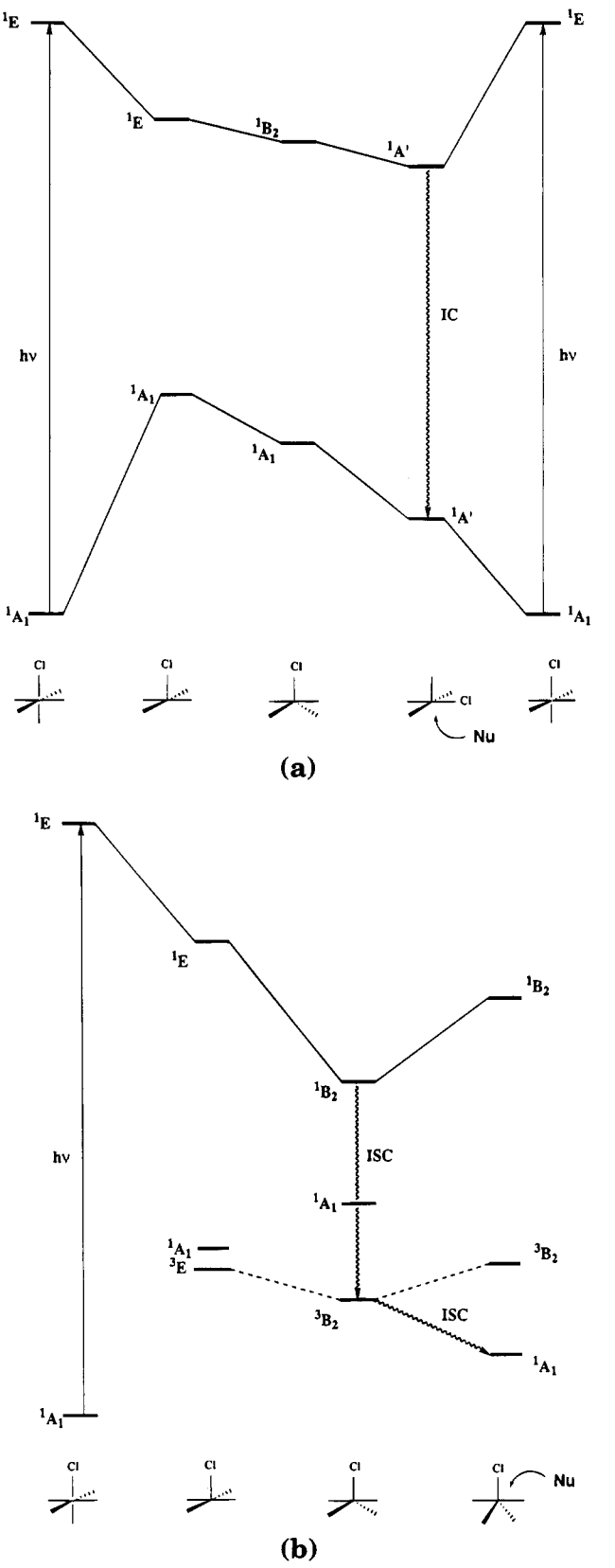

Figure 1. State correlation diagrams corresponding to the mechanisms proposed (a) by DV[2] and (b) by PHV[3] for reaction 2.

the degree of electron correlation may also be responsible for this situation. In the work of DV, electron correlation was partly included through a limited CI. The study of PHV does not go beyond the SCF level. It is generally agreed that SCF theory yields only qualita-

Scheme 1

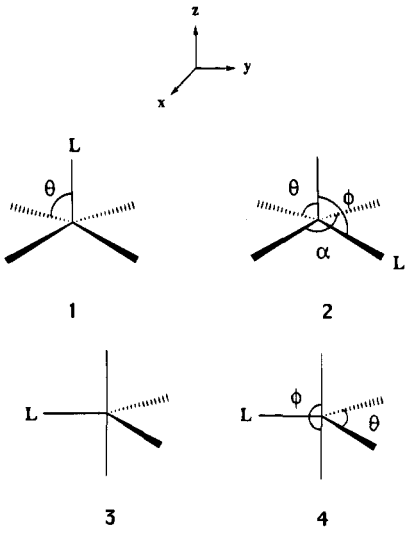

tive results for the excited states of organometallics[7] and the good agreement obtained by PHV between the calculated excitation energies of $Mn(CO)_5Cl$ and the experimental values should be considered as rather fortuitious.

We report here a theoretical study of the mechanism of the primary photoprocess (reaction 2). As in our previous study, we consider the possible excited-state isomerization pathways of the five-coordinate species $M(CO)_4L$. More specifically, we try to assess (i) the influence of the correlation effects on the results obtained for $Mn(CO)_4Cl$.[6] [This has been achieved by performing CASSCF/CASPT2 calculations of the relative stabilities of the different structures of $Mn(CO)_4Cl$ in the lowest excited states (singlet and triplet).] and (ii) the effect of enlarging the basis set on the results obtained for $Tc(CO)_4Cl$ and $Mo(CO)_4NH_3$. [The basis set effect on the relative stabilities of the different structures of $Tc(CO)_4Cl$ and $Mo(CO)_4NH_3$ has been ascertained at the SCF level with double-ζ quality basis sets.]

The results obtained for $Mn(CO)_4Cl$ have been used to build a state correlation diagram that connects the ground state and lowest excited states of the reactant $Mn(CO)_5Cl$ with those of the five-coordinate species $Mn(CO)_4Cl$ in the various structures (SP with L basal or apical, TBP, and d-TBP). On the basis of this state correlation diagram, we propose a qualitative mechanism for the photosubstitution reaction which has been improved over the one proposed previously[2] and which accounts for the cis-stereospecificity of reaction 1.

The Calculations

The calculations were carried out for the five-coordinate systems $Mn(CO)_4Cl$, $Tc(CO)_4Cl$, and $Mo(CO)_4NH_3$ with the conformations **1** (SP with L in apical position, C_{4v} symmetry), **2** (SP with L in basal position, C_s symmetry), **3** (regular TBP, C_{2v} symmetry) and **4** (d-TBP, C_{2v}) (Scheme 1). The ligand−metal−ligand bond angles were optimized at the SCF level for the lowest singlet and triplet states of $Mn(CO)_4Cl$ and the lowest singlet states of $Tc(CO)_4Cl$ and $Mo(CO)_4NH_3$ with the following bond lengths (these bond lengths were taken from the previous calculations[2,3] and retained in the subsequent calculations): for $Mn(CO)_4Cl$, Mn−Cl = 2.369 Å, Mn−C = 1.841 Å, C−O = 1.124 Å; for $Tc(CO)_4Cl$, Tc−Cl = 2.400 Å, Tc−C = 1.950 Å, C−O = 1.150 Å; for $Mo(CO)_4NH_3$, Mo−N = 2.200 Å, Mo−C = 2.000 Å, C−O = 1.150 Å, N−H = 1.012 Å, HNH = 106.7°.

Table 1. Total CASSCF Energy (in au and Relative to −2059) for the Lowest Singlet and Triplet States of $Mn(CO)_4Cl$

structure	point group	state	main configuration	active space	total energy
SP apical	C_{4v}	$^1A_1$	$(3d_{xz})^2(3d_{yz})^2(3d_{xy})^2$	6e6a	0.960 68
		^3E	$(3d_{xz})^{3/2}(3d_{yz})^{3/2}(3d_{xy})^2(3d_{z^2})^1$	6e7a	0.942 80
		^1E	$(3d_{xz})^{3/2}(3d_{yz})^{3/2}(3d_{xy})^2(3d_{z^2})^1$	6e7a	0.897 88
TBP	C_{2v}	$^1A_1$	$(3d_{xz})^2(3d_{yz})^2(3d_{x^2-y^2})^2$	6e6a	0.970 68
		$^3B_2$	$(3d_{xz})^2(3d_{yz})^2(3d_{x^2-y^2})^1(3d_{xy})^1$	6e7a	0.927 09
		$^1B_2$	$(3d_{xz})^2(3d_{yz})^2(3d_{x^2-y^2})^1(3d_{xy})^1$	6e7a	0.887 62
		$^3A_2$	$(3d_{xz})^2(3d_{yz})^1(3d_{x^2-y^2})^2(3d_{xy})^1$	6e7a	0.929 12
		$^1A_2$	$(3d_{xz})^2(3d_{yz})^1(3d_{x^2-y^2})^2(3d_{xy})^1$	6e7a	0.870 63
d-TBP	C_{2v}	$^1A_1$	$(3d_{xz})^2(3d_{yz})^2(3d_{x^2-y^2})^2$	6e6a	0.991 33
		$^3B_2$	$(3d_{xz})^2(3d_{yz})^2(3d_{x^2-y^2})^1(3d_{xy})^1$	6e7a	0.930 17
		$^1B_2$	$(3d_{xz})^2(3d_{yz})^2(3d_{x^2-y^2})^1(3d_{xy})^1$	6e7a	0.890 71
		$^3A_2$	$(3d_{xz})^2(3d_{yz})^1(3d_{x^2-y^2})^2(3d_{xy})^1$	6e7a	0.929 86
		$^1A_2$	$(3d_{xz})^2(3d_{yz})^1(3d_{x^2-y^2})^2(3d_{xy})^1$	6e7a	0.870 56
SP basal	C_s	$^1A'$	$(3d_{xz})^2(3d_{yz})^2(3d_{xy})^2$	6e6a	0.980 83
		$^3A'$	$(3d_{xz})^2(3d_{yz})^1(3d_{xy})^2(3d_{z^2})^1$	6e7a	0.928 34
		$^1A'$	$(3d_{xz})^2(3d_{yz})^1(3d_{xy})^2(3d_{z^2})^1$	6e7a	0.884 84

We have used the following Gaussian basis sets: for manganese, a (15, 11,6) set contracted to [9, 6, 3];[8] for molybdenum and technicium, a (17, 13, 9) set contracted to [11, 8, 6];[11] for chlorine, a (12, 9) set contracted to [6, 4];[14] for the first-row atoms, a (10, 6) set contracted to [4, 2];[15] for hydrogen, a (5) set contracted to [2][16] (basis sets I). A second series of reference calculations has been performed on $Mn(CO)_4Cl$ using generally contracted ANO (atomic natural orbital) basis sets:[17] for manganese, a (17, 12, 9, 4) set contracted to [5, 4, 3, 1]; for chlorine, a (13, 10, 4) contracted to [6, 4, 2]; and for the first-row atoms, a (10,6,3) set contracted to [3, 2, 1][18] (basis sets II).

CASSCF calculations[19] were carried out, using basis sets I for a number of low-lying excited states of the system $Mn(CO)_4Cl$, for the two (apical and basal) SP and the two (regular and distorted) TBP structures, with the geometries optimized at the SCF level. For the singlet excited states, we have used the geometries optimized for the corresponding triplet states. The details of these CASSCF calculations are given in Table 1. The active space for each calculation is made of the occupied 3d orbitals of the Mn atom and of the 4d

(7) Veillard, A. *Chem. Rev.* **1991**, *91*, 743.

(8) This basis set, derived from the basis set given by Wachters,[9] has been described in ref 10.

(9) Wachters, A. J. H. *J. Chem. Phys.* **1970**, *52*, 1033.

(10) Veillard, A.; Rohmer, M-M. *Int. J. Quant. Chem.* **1992**, *42*, 965.

(11) The (17, 13, 9) set of Mo and Tc is derived from the (17, 11, 8) basis set of Huzinaga[12] by adding two diffuse p functions and one diffuse d function, with their exponents chosen according to the even-tempered criterion.[13]

(12) Huzinaga, S. *J. Chem. Phys.* **1977**, *66*, 4245.

(13) Raffenetti, R. C.; Bardo, R. D.; Ruedenberg, K. In *Energy, Structure and Reactivity*; Smith, D. W., McRae, W. B., Eds.; Wiley: New York, 1973; p 164.

(14) Veillard, A. Theoret. Chim. Acta **1968**, *12*, 405.

(15) Huzinaga, S. *Approximate Atomic Functions*; Technical Report, University of Alberta: Alberta, 1971.

(16) Huzinaga, S. J. *Chem. Phys.* **1965**, *42*, 1293.

(17) Almlof, J.; Taylor, P. R. *J. Chem. Phys.* **1987**, *86*, 4070.

(18) Pierloot, K.; Dumez, B.; Widmark, P.-O.; Ross, B. O. *Theor. Chim. Acta*, in press.

(19) Siegbahn, P. E. M.; Almlof, J.; Heiberg, A.; Roos, B. *J. Chem. Phys.* **1981**, *74*, 2384.

Table 2. Optimized Angles and Total SCF Energies (in au and Relative to −2059) for the Low-Lying Singlet and Triplet States of $Mn(CO)_4Cl$

structure	state	electronic configuration	optimized angles θ	φ	α	total energy
SP apical	$^1A_1$	$(16a_1)^2(1a_2)^2(6b_1)^2(2b_2)^2(12e)^4$	88°			0.831 16
	^3E	$(17a_1)^1(1a_2)^2(6b_1)^2(2b_2)^2(12e)^3$	92°			0.833 55
TBP[a]	$^1A_1$	$(23a_1)^2(3a_2)^2(12b_1)^2(11b_2)^2$				0.826 34
	$^3B_2$	$(23a_1)^1(3a_2)^2(12b_1)^2(12b_2)^1$				0.835 12
	$^3A_2$	$(23a_1)^2(3a_2)^2(12b_1)^1(12b_2)^1$				0.828 07
d-TBP	$^1A_1$	$(23a_1)^2(3a_2)^2(12b_1)^2(11b_2)^2$	95°	170°		0.845 36
	$^3B_2$	$(23a_1)^1(3a_2)^2(12b_1)^2(11b_2)^1$	140°	172°		0.840 87
	$^3A_2$	$(23a_1)^2(3a_2)^2(12b_1)^1(12b_2)^1$	126°	185°		0.828 87
SP basal	$^1A'$	$(34a')^2\ (15a'')^2$			*b*	0.835 45
	$^3A'$	$(34a')^1\ (35a')^1\ (15a'')^2$	98°	101°	170°	0.835 28

[a] $\theta = 120°$; $\varphi = 180°$. [b] $\theta = \varphi = 90°$; $\alpha = 180°$ (assumed).

orbitals which correlate to the 3d orbitals doubly occupied in the closed-shell configuration. The six electrons from the 3d orbitals were correlated. The integral calculations were carried out with the ASTERIX[20] system of programs. In order to study the convergence of basis sets and correlation effects, a series of reference CASSCF calculations, using basis sets II (ANO), has been performed for a number of low-lying excites states of the different structures of the system $Mn(CO)_4Cl$. Six electrons were correlated in eight active orbitals in these calculations. Remaining correlation effects have been treated with the second-order perturbation CASPT2 method,[21] the full CASSCF space generating the reference configurations. These reference calculations were carried out with the MOLCAS-2 software.[22]

Results and Discussion

Geometry Optimization and SCF Results. In Table 2, we have reported the optimized values of the angles and the corresponding SCF energies for the low-lying singlet and triplet states of $Mn(CO)_4Cl$. The corresponding relative energies are presented in Table 3 together with the results of PHV.

The optimized values for the angle θ of the SP apical are 88° and 92° for the lowest singlet and triplet states, respectively (PHV used an idealized value of 90°). For the distorted TBP in the $^1A_1$ state, our optimized values of $\theta = 95°$ and $\varphi = 170°$ are close to the values obtained by PHV ($\theta = 95°$, $\varphi = 172°$). Optimization of the angles for the SP basal in the $^1A'$ state yielded the distorted TBP structure, and the energy values reported in Tables 2 and 3 for the SP basal have been obtained with the assumed values $\theta = \varphi = 90°$, $\alpha = 180°$. Finally, one may notice for the distorted TBP a large difference in the values of the angle θ optimized for the singlet (95°) and for the triplet states ($\theta = 140°$ for the $^3B_2$ state and $\theta = 126°$ for the $^3A_2$ state). Thus the angle θ increases by 45° when going from the $^1A_1$ state to the $^3B_2$ state (corresponding to the electronic excitation $d_{x^2-y^2} \rightarrow d_{xy}$). When the d_{xy} orbital is populated, some stabilization is gained by increasing θ through the bonding interaction **5** with the equatorial carbonyl ligands. PHV used for the triplet states the value of the angle θ optimized for the $^1A_1$ state.

Table 3. Relative Energies (in kcal mol^{-1}) for the Different Structures of $Mn(CO)_4Cl$ in the Lowest Singlet and Triplet States (a) from This Work and (b) from PHV

structure	state	SCF this work	SCF PHV[a]	CASSCF[b] this work	CASPT2[c] this work
SP apical	$^1A_1$	8.9	10.0	19.2 (21.2)	21.5
	^3E	7.4	8.9	30.4 (25.0)	15.6
TBP	$^1A_1$	11.9	12.9	12.9 (13.2)	15.2
	$^3B_2$	6.4	6.3	40.3 (30.9)	4.1
	$^3A_2$	10.8	11.7	39.0	
d-TBP	$^1A_1$	0.0	0.0	0.0 (0.0)	0.0
	$^3B_2$	2.8	8.4	38.4 (30.0)	2.7
	$^3A_2$	10.3	17.7	38.6	
SP basal	$^1A'$	6.2	5.7	6.6 (6.3)	3.0
	$^3A'$	6.3	16.0	39.6 (18.7)	9.9

[a] Approximate values from Figure 3 of ref 3. [b] The values in parentheses correspond to the CASSCF results obtained with basis sets II (ANO). [c] Values with basis sets II (ANO) on the top of CASSCF with six electrons correlated in eight active orbitals.

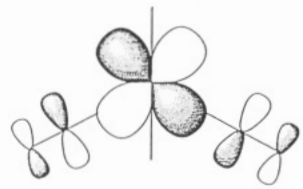

5

At the SCF level, the most stable structure is the distorted TBP in the $^1A_1$ state. This greater stability of the distorted TBP has already been discussed in DV. For the two SP structures, the lowest singlet and triplet states are nearly degenerate at the SCF level. This was also the case in PHV, at least for the SP apical. However, one should keep in mind that, because of the lack of correlation at the SCF level, the triplet states are artificially stabilized relatively to the closed-shell singlet state. For the regular TBP the $^3B_2$ state appears to be the ground state at the SCF level.

The angles optimized for the lowest singlet states of $Tc(CO)_4Cl$ and $Mo(CO)_4NH_3$ and the corresponding SCF energies are reported in Table 4. The relative energies are given in Table 5 together with the results of our previous study[2] using idealized geometries and smaller basis sets. The trends in Table 5 are rather similar for these two species. The distorted TBP and the SP basal are close in energy, the most stable structure being the distorted TBP for $Tc(CO)_4Cl$ (as it was the case for $Mn(CO)_4Cl$) but the SP basal for $Mo(CO)_4NH_3$. The relative stability of the TBP and of the distorted TBP are similar in this work and in DV, thus this result is relatively insensitive to the size of the basis set (the optimized value of θ in this study being extremely close to the value of 90° assumed by DV). On the contrary, the results of Table 5 show a significant stabilization of the two SP structures in this work when compared to the results of DV. This is a consequence of the fact that DV assume a value of 100° for the angle θ, which is rather different from the optimized values 88°−90° of this work. We obtained with the present basis set a SCF energy of −5114.585 au for $Tc(CO)_4Cl$ in the SP

(20) Ernenwein, R.; Rohmer, M. M.; Benard, M. *Comp. Phys. Commun.* **1990**, *58*, 305.
(21) Andersson, K.; Malmqvist, P.-A.; Roos, B. O.; Sadlej, A. J.; Wolinski, K. J. *Phys. Chem.* **1990**, *94*, 5483. Andersson, K.; Malqvist, P.-A.; Roos, B. O. *J. Chem. Phys.* **1992**, *96*, 1218.
(22) Andersson, K.; Blomberg, M. R. A.; Fülscher, M. P.; Kellö, V.; Lindh, R.; Malmquist, P. A.; Noga, J.; Olsen, J.; Roos, B. O.; Sadlej, A. J.; Siegbahn, P. E. M.; Urban, M.; Widmark, P.-O. *MOLCAS*, Version 2.0, University of Lund: Sweden, 1991.

Table 4. Optimized Angles and Total SCF Energies (in au) for the Lowest Singlet States of $Tc(CO)_4Cl$ and $Mo(CO)_4NH_3$

	structure	point group	state	electronic confign	θ	φ	α	total energy
$Tc(CO)_4Cl$	SP apical	C_{4v}	$^1A_1$	$(19a_1)^2(1a_2)^2(7b_1)^2(3b_2)^2(14e)^4$	88°			−5114.631 60
	TBP	C_{2v}	$^1A_1$	$(27a_1)^2(4a_2)^2(14b_1)^2(13b_2)^2$				−5114.620 76
	d-TBP	C_{2v}	$^1A_1$	$(27a_1)^2(4a_2)^2(14b_1)^2(13b_2)^2$	89°	174°		−5114.657 98
	SP basal	C_s	$^1A'$	$(40a')^2(18a'')^2$		*a*		−5114.654 91
$Mo(CO)_4NH_3$	SP apical	C_s	$^1A'$	$(37a')^2(17a'')^2$	90°			−4482.024 29
	TBP	C_s	$^1A'$	$(38a')^2(16a'')^2$				−4482.004 74
	d-TBP	C_s	$^1A'$	$(38a')^2(16a'')^2$	87°	182°		−4482.044 11
	SP basal	C_s	$^1A'$	$(37a')^2(17a'')^2$	90°	100°	181°	−4482.048 90

Table 5. Relative SCF Energies (in kcal mol^{-1}) of the Singlet States of the SP and TBP Structures for the Systems $M(CO)_4L$ from (a) This Work, (b) Reference 2, and (c) Reference 3

		SPap	TBP	d-TBP	SPbas
$Tc(CO)_4Cl$	a	16.6	23.4	0.0	1.9
	b	49.0	23.0	0.0	9.0
$Mo(CO)_4NH_3$	a	15.5	27.7	3.0	0.0
	b	31.0	24.0	0.0	8.0
$Mn(CO)_4Cl$	a	8.9	11.9	0.0	6.2
	c	10.0	12.9	0.0	5.7

Table 6. Total CASSCF and CASPT2 Energies (in au and Relative to −2060 and −2062, Respectively) for the Lowest Singlet and Triplet States of $Mn(CO)_4Cl$

structure	point group	state	main configuration	CASSCF	CASPT2
SP apical	C_{4v}	$^1A_1$	$(3d_{xz})^2(3d_{yz})^2(3d_{xy})^2$	0.40032	0.25260
		^3E	$(3d_{xz})^{3/2}(3d_{yz})^{3/2}(3d_{xy})^2(3d_{z^2})^1$	0.39427	0.26191
		^1E	$(3d_{xz})^{3/2}(3d_{yz})^{3/2}(3d_{xy})^2(3d_{z^2})^1$	0.35706	0.22733
TBP	C_{2v}	$^1A_1$	$(3d_{xz})^2(3d_{yz})^2(3d_{x^2-y^2})^2$	0.41291	0.26252
		$^3B_2$	$(3d_{xz})^2(3d_{yz})^2(3d_{x^2-y^2})^1(3d_{xy})^1$	0.38493	0.28021
		$^1B_2$	$(3d_{xz})^2(3d_{yz})^2(3d_{x^2-y^2})^1(3d_{xy})^1$	0.35101	0.24889
d-TBP	C_{2v}	$^1A_1$	$(3d_{xz})^2(3d_{yz})^2(3d_{z^2-y^2})^2$	0.43412	0.28680
		$^3B_2$	$(3d_{xz})^2(3d_{yz})^2(3d_{x^2-y^2})^1(3d_{xy})^1$	0.38626	0.28254
		$^1B_2$	$(3d_{xz})^2(3d_{yz})^2(3d_{x^2-y^2})^1(3d_{xy})^1$	0.35231	0.25309
SP basal	C_s	$^1A'$	$(3d_{xz})^2(3d_{yz})^2(3d_{xy})^2$	0.42414	0.28208
		$^3A'$	$(3d_{xz})^2(3d_{yz})^1(3d_{xy})^2(3d_{z^2})^1$	0.40438	0.27103
		$^1A'$	$(3d_{xz})^2(3d_{yz})^1(3d_{xy})^2(3d_{z^2})^1$	0.36957	0.23798

apical structure with $\theta = 100°$; this gives a relative energy of 46 kcal mol^{-1}, in fair agreement with the value of 49 kcal mol^{-1} reported by DV. The most stable structure of $Tc(CO)_4Cl$ is the distorted TBP in the $^1A_1$ state as was already the case for $Mn(CO)_4Cl$, but the destabilization of the SP basal has been much reduced (1.9 kcal mol^{-1} for $Tc(CO)_4Cl$ vs 6.2 kcal mol^{-1} for $Mn(CO)_4Cl$). As for $Mn(CO)_4Cl$, optimization of the angles for the SP basal in the $^1A'$ state resulted in the distorted TBP structure. For $Mo(CO)_4NH_3$ the most stable structure turns out to be the SP basal rather than the distorted TBP.

CASSCF/CASPT2 Calculations for $Mn(CO)_4Cl$. We have reported in Table 1 the CASSCF results for the lowest singlet and triplet states of $Mn(CO)_4Cl$ in the four structures, using basis sets I. The total CASSCF energies obtained with basis sets II (ANO) are reported in Table 6, together with the total CASPT2 energies for a number of low-lying electronic states of $Mn(CO)_4Cl$ involved in the mechanism of reaction 2. The comparison among our SCF results, those of PHV, the CASSCF results with basis sets I or basis sets II and the CASPT2 results is made in Table 3. The CASSCF treatment does not change drastically the relative order of the different structures with closed-shell states, the correlation energy recovered being in the range 0.13−0.15 au for all these states. The distorted TBP in the $^1A_1$ state is more stable than the SP basal by 6.6 kcal mol^{-1} (the SCF value was 6.2 kcal mol^{-1}). The relative order of the SP apical and of the regular TBP in the $^1A_1$ state is reversed at the CASSCF level, the regular TBP being now more stable by 6.3 kcal mol^{-1} (it was less stable by 3 kcal mol^{-1} at the SCF level). Compared to the closed-shell states, the triplet states are artificially stabilized at the SCF level since the pair correlation is not included. Consequently, at the CASSCF level, the low-lying triplet states are now well above the closed-shell singlet states. The comparison between the CASSCF results using basis sets I and II shows convergence of basis sets effects. Indeed, the use of ANO basis sets does not change drastically the relative order of the four structures in the different electronic states. If the relative energies of the lowest closed-shell singlet states of $Mn(CO)_4Cl$ in the different structures are not modified by the remaining correlation effects, the relative order of the electronic states corresponding to open-shell configurations (singlet or triplet) is considerably affected by a more accurate calculation (CASPT2 results). It may be explained by the fact that, in the CASSCF calculations, including six electrons correlated in six to eight orbitals, three pairs of electrons are correlated in the lowest singlet states, whereas only two pairs are correlated in the open-shell configurations. The CASPT2 tends to restore this unbalanced description of the correlation effects. The main consequence of a more refined treatment is the stabilization of the lowest triplet states for the four different structures, the trigonal bipyramid isomers (regular and distorted TBP) becoming more stable than the two square pyramid structures (basal and apical). The singlet excited states follow the same trends as the corresponding triplet states. From the results reported in Tables 3 and 6, we may draw the following conclusions: (i) the distorted TBP either in the $^1A_1$ state or in the $^3B_2$ state is more stable than the other structures for $Mn(CO)_4Cl$ or nearly degenerate with the SP basal in the $^1A'$ state; (ii) the low-lying triplet states are not expected to play a key role in the late stage of the photosubstitution, namely the nucleophilic attack of an incoming ligand L′ (reaction 3); (iii) the mechanism of the photosubstitution may depend slightly on the metal center, the reactive species being the distorted TBP for Mn and Tc but the SP basal for Mo; (iv) the distorted TBP in the $^1A_1$ state and the SP basal in the $^1A'$ state are the best candidates for the nucleophilic attack.

The Mechanism of the Nucleophilic Addition (Reaction 3). From the above results, there are two structures which are likely candidates for the nucleophilic attack (3), namely the SP basal and the distorted TBP. The attack of an incident nucleophile L′ on a SP basal (Scheme 2) is a well-documented reaction which is favored both on steric grounds and in terms of

Table 7. Optimized Angles (in deg) and SCF Energies (in au, Relative to −2102) along the Potential Energy Curve for the Reaction *cis*-$Mn(CO)_4Cl(NH_3) \rightarrow Mn(CO)_4Cl + NH_3$ as a Function of the Distance Mn−N (in Å)

d	2.069	2.569	3.0	3.5	4.0	5.0	7.0	9.0	OO
β	91.61	95.52	100.45	104.61	117.08	130.03	130.71	130.75	130.45
φ	90.85	92.35	92.50	92.36	91.40	90.54	90.33	90.25	90.37
θ	85.66	85.50	85.47	85.64	85.65	85.68	85.58	85.61	85.62
α	−2.76	−0.45	3.64	7.63	20.86	36.34	36.87	36.99	36.66
E	0.66882	0.66138	0.64682	0.63291	0.62138	0.61044	0.60758	0.60728	0.60704

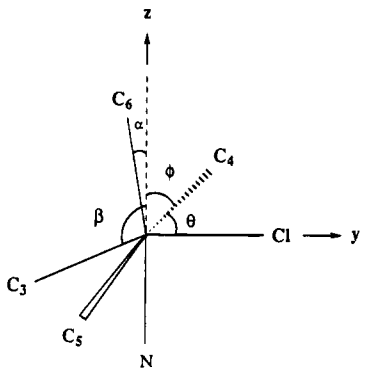

Figure 2. The angles defining the geometry of the system *cis*-$Mn(CO)_4Cl(NH_3)$.

Scheme 2

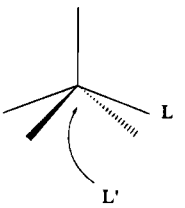

Scheme 3

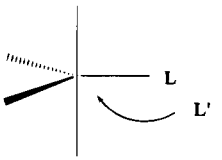

HOMO−LUMO interaction.[23-24] The attack of an incoming nucleophile in the equatorial plane of a distorted TBP (Scheme 3) might be energetically less favorable and the occurrence of a transition state with an energy barrier cannot be ruled out at first. In that case a rearrangement of the distorted TBP to the SP basal as the first step of the reaction might be energetically more favorable. In order to clear out these points, one possibility would be to compute the energy profiles for the two schemes, 2 and 3. However we have used the principle of microscopic reversibility[25] and we have calculated the energy profile of the reverse reaction

$$cis\text{-}Mn(CO)_4Cl(NH_3) \rightarrow Mn(CO)_4Cl + NH_3 \quad (4)$$

with the energy gradient technique at the SCF level (the basis set used was of the STO-3G type for the first and second row atoms and of a split valence type for the metal atom). The corresponding energy values together with the optimized values of the angles (as defined in Figure 2) are reported as a function of the Mn−N distance in Table 7 (the other bond lengths were assumed to remain constant along the reaction path). The results of Table 7 show that, at the end of the reaction 4, $Mn(CO)_4Cl$ has the structure of a distorted TBP and that this has been achieved without any barrier along the reaction path. We conclude that the distorted TBP in the $^1A_1$ state is probably the reactive species of the nucleophilic addition which occurs without energy barrier. However, according to the small energy gap between the d-TBP $^1A_1$ and the SP basal $^1A'$ (of the order of 3.0 kcal/mol), experimental factors like low-temperature effects or solvation phenomena may favor one or the other sructure.

The Mechanism of the Photosubstitution Reaction. Our analysis of the mechanism of the photosubstitution for d^6 metal carbonyls $M(CO)_5L$ will be based on the state correlation diagram connecting the ground and lowest excited states of the model system $Mn(CO)_5Cl$ and of the five-coordinate species $Mn(CO)_4Cl$ in the various structures, with the assumption that the photochemical reaction (1) results from the primary photodissociation of a carbonyl (reaction 2) followed by a subsequent nucleophilic addition (reaction 3).

We shall consider both axial and equatorial departure of the carbonyl ligand in reaction 1. Indeed, there is no experimental evidence regarding which of the carbonyls is eliminated. For $W(CO)_5CS$, it was found that the loss of an axial or equatorial carbonyl is equally probable.[26] According to PHV, excitation of $Mn(CO)_5Cl$ into the lowest ligand field (LF) state,$^{1,3}E$, should favor the elimination of an axial carbonyl ligand while excitation into the higher LF state,$^{1,3}A_2$, would result in the elimination of an equatorial ligand. However these conclusions are based solely on electron density difference plots and population analysis for the reactant. In order to reach firmer conclusions on the relative importance of axial and equatorial elimination, it would be necessary to study the dynamics of these photodissociations and this would require a detailed knowledge of the corresponding potential energy surfaces.[27]

On the basis of a state correlation diagram (Figure 3) based upon the CASPT2 results of Table 6, we propose the following mechanism for the photosubstitution of the axial carbonyl in $Mn(CO)_5Cl$ (left side of Figure 3): (i) excitation of $Mn(CO)_5Cl$ into the ^1E ligand field state is followed by elimination of the axial carbonyl ligand with formation of $Mn(CO)_4Cl$ as a SP apical in the ^1E state; (ii) from there $Mn(CO)_4Cl$ evolves along a Berry pseudorotation path to the $^1B_2$ of the regular TBP; (iii) an *internal conversion* brings the system to the $^1A_1$ ground state of the regular TBP; (iv) after a downhill rearrangement, the molecule gets

(23) Elian, M.; Hoffmann, R. *Inorg. Chem.* **1975**, *14*, 1058.
(24) Pearson, R. G. *Symmetry rules for chemical reactions*; J. Wiley: New-York, 1976.
(25) Jackson, W. G. *Inorg. Chem.* **1987**, *26*, 3004.
(26) Poliakoff, M. *Inorg. Chem.* **1976**, *15*, 2892.
(27) Daniel, C.; Heitz, M. C.; Lehr, L.; Schröder, T.; Warmuth, B. *Int. J. Quant. Chem.* **1994**, *52*, 71. Daniel, C.; Heitz, M. C.; Lehr, L.; Manz, J.; Schröder, T. *J. Phys. Chem.* **1993**, *97*, 12485. Daniel, C.; Kolba, E.; Lehr, L.; Manz, J.; Schröder, T. *J. Phys. Chem.* **1994**, *98*, 9823.

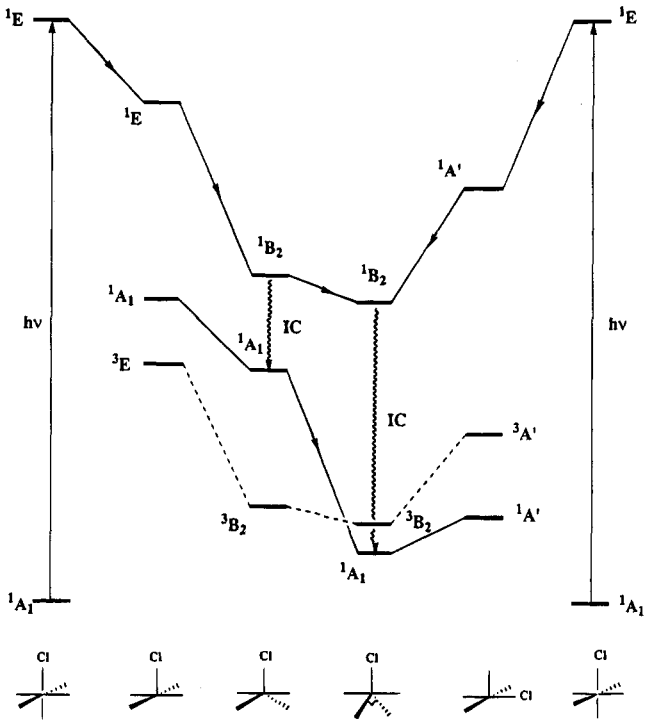

Figure 3. State correlation diagram for the photoelimination of the axial carbonyl ligand (left side) and of the equatorial carbonyl ligand (right side) from $Mn(CO)_5Cl$.

trapped in the potential well corresponding to the $^1A_1$ ground state of the distorted TBP, until it reacts with an incident nucleophile.

Should the photosubstitution lead to the loss of an equatorial carbonyl, the mechanism would be (right side of Figure 3) as follows: (i) excitation of $Mn(CO)_5Cl$ into the ^1E ligand field state is followed by elimination of the equatorial carbonyl ligand with formation of $Mn(CO)_4Cl$ as a SP basal in the $^1A'$ state; (ii) from there the system evolves to the distorted TBP in the $^1B_2$ state; (iii) the system gets trapped, through an *internal conversion*, into the $^1A_1$ ground state of the distorted TBP.

This qualitative mechanism accounts for the cis stereospecificity of the photosubstitutions in d^6 metal carbonyls. It differs slightly from the mechanism proposed by DV by two points: (i) in both cases (axial or equatorial elimination), internal conversion now takes place after the rearrangement to the TBP structures; (ii) the reactive species would be the distorted TBP rather than the SP basal, at least for $Mn(CO)_4Cl$ and $Tc(CO)_4Cl$. This may not be the case for $Mo(CO)_4NH_3$ for which the reactive species may be the SP basal. This requires only a minor modification of the state correlation diagram and little change in the reaction mechanism.

We believe that the lowest triplet states do not play any role in this mechanism since the *intersystem crossing* processes $^1E \rightarrow {}^3E$ (SP apical) or $^1A' \rightarrow {}^3A'$ (SP basal) should be less favorable than the rearrangements to the TBP structures regarding the large singlet–triplet energy gap (greater than 1 eV). For the same reason, the $^1B_2 \rightarrow {}^3B_2$ (TBP or d-TBP) *intersystem crossings* seem to be unlikely. Indeed, we have shown in a recent dynamical study[28] that the fast (<50 ps) spin–orbit induced radiationless transitions in organometallics, competitive with dissociation or downhill rearrangements on steep potential energy surfaces, occur at critical geometries (crossing points). The only probable singlet–triplet transition in the diagram of Figure 3 is the $^3B_2 \rightarrow {}^1A_1$ (distorted-TBP) *intersystem crossing* which is symmetry allowed and metal-centered and which occurs between two nearly degenerate states.[28,29] Consequently, the role of this triplet state is not excluded in the mechanism of photosustitution of complexes with heavy metal atoms.

Acknowledgment. The calculations have been carried out on the Cray-2 computer of the CCVR (Palaiseau, France), on the IBM 3090 of the CCSC (Strasbourg, France) and on the IBM RS 6000 workstations of the laboratory. The authors are grateful to B. O. Roos for making available ANO basis sets prior to publication. T.M. thanks the French Ministère des Affaires Etrangères for a fellowship.

OM940401L

(28) Daniel, C.; Heitz, M. C.; Manz, J.; Ribbing, C. *J. Phys. Chem.*, in press.
(29) Ribbing, C.; Daniel, C. *J. Chem. Phys.* **1994**, *100*, 6591.